The Vibration Isolation Properties of an Asymmetrical Quasi-Zero Stiffness Isolator with Geometrical Nonlinear Damping

Chuanyun Yu and Jianrun Zhang*
School of Mechanical Engineering, Southeast University, Nanjing, China
Email: zhangjr@seu.edu.cn (C.Y.), 230218041@seu.edu.cn (J.Z.)

***Abstract*—This paper proposes a Quasi-Zero-Stiffness (QZS) vibration isolator with asymmetric stiffness and geometric nonlinear damping. The nonlinear stiffness and nonlinear damping characteristics of proposed model are studied. The motion equation of proposed system under force excitation is established, and its dynamic response is solved by the Harmonic Balance Method (HBM). In addition, the influence of nonlinear damping on force transmissibility is studied. The results indicate that the proposed isolator has a large equivalent damping ratio in the resonance region and a small equivalent damping ratio in the high-frequency region. Therefore, the proposed asymmetrical QZS isolator with nonlinear damping can supress the resonance in low-frequency under force excitation and achieve a good high-frequency vibration isolation effect simultaneously than that with linear damping.**

***Index Terms*—quasi-zero stiffness, geometrical nonlinear damping, vibration isolation, asymmetrical stiffness**

I. Introduction

Low-frequency vibration phenomenon is ubiquitous in industrial environments, which will reduce the reliability of precision equipment. Reducing the stiffness can effectively increase the vibration isolation frequency band for linear vibration isolators. However, the decrease in system stiffness also means a decrease in bearing capacity, which limits the application of linear systems in low-frequency vibration isolation. Fortunately, nonlinear vibration isolators with high-static and low-dynamic stiffness (HSLDS) characteristics can overcome this problem and have attracted extensive attention [1].

Due to the nonlinear stiffness properties, quasi-zero-stiffness (QZS) isolator is easy to jump when the excitation amplitude is large, which seriously affect its vibration isolation performance [2]. Increasing damping can effectively suppress the resonance and jump of QZS isolator, but it will reduce the high-frequency vibration isolation performance. Therefore, nonlinear damping has been studied to overcome this problem [3]. Previous studies mainly focused on the effect of geometrical nonlinear damping on QZS isolator with symmetric stiffness characteristics, ignoring that with asymmetric stiffness characteristics [4]. As a result, this paper proposes a QZS isolator with asymmetric stiffness and geometric nonlinear damping, and investigates the influence mechanism of nonlinear damping on its vibration isolation performance under force excitation. The results indicates that the proposed QZS isolator can supress the resonance in low-frequency and achieve a good high-frequency vibration isolation effect simultaneously than linear damping.

Manuscript received January 10, 2024; revised February 25, 2024; accepted March 15, 2024.
*Corresponding author

II. Literature Review

Through the exploration and utilization of nonlinear characteristics, QZS isolator is proposed by researchers to realize low-frequency vibration isolation. QZS isolator is usually composed of positive and negative stiffness mechanisms in parallel [5]. Carella [6] connects a group of oblique springs with vertical springs to construct a classic three-spring QZS isolator. The stiffness of the isolator is close to zero at the equilibrium position, which can achieve good low-frequency vibration isolation effect. With the deepening of research, more negative stiffness structures are proposed, including cam-rollers [7], magnets [8], electromagnetics [9], buckling beams [10] and so on [11], [12]. Inspired by the nonlinear characteristics of animal limbs, Jing [13, 14] proposed a kind of X-shaped mechanism with QZS properties, which is simple in structure and beneficial to engineering application. Up to now, a large number of research results have been reported on X-shaped mechanisms under displacement excitation, including asymmetric structures [15], scissors-like structures [16] and multi-layer structures [17]. Moreover, in order to achieve better low-frequency vibration isolation effect, not only the nonlinear stiffness has been widely investigated, but also the nonlinear damping characteristics, such as cubic damping and horizontal geometric nonlinear damping [18, 19]. Cheng [3] proposes geometric nonlinear damping and applies it to QZS system to improve the vibration suppression performance in low frequency region. Dong [20] designs a semi-active electromagnetic shunt damping as geometrically nonlinear damping. Liu [21] studies the influence of nonlinear damping on typical QZS systems. Overall, it is an important research purpose to improve the vibration isolation performance of QZS isolator through nonlinear damping.

doi: 10.18178/ijeetc.13.4.304-308

III. Modelling and Static Analysis

The structural diagram of the proposed QZS isolator is shown in Fig. 1. In Fig. 1(a), four rods and a slide rail are installed between the support platform and the base, and the rods are connected by joints. A horizontal spring and damper are installed between the end blocks to provide negative stiffness and nonlinear damping. The slide rail is fixed on the base, and the support table can move vertically along the slide rail. Meanwhile, a vertical spring is sleeved on the slide rail to provide positive stiffness. The isolated mass m is placed on the support platform to realize vibration isolation. Fig. 1(b) shows the geometric deformation relationship of the proposed model under the action of force *F*. Ignoring the length of the end block and the elastic deformation of the rods, the following geometric relationship can be obtained as

$$x = 2L\cos\theta - 2L\cos\theta_0 \tag{1}$$

$$y = 2L\sin\theta_0 - 2L\sin\theta \tag{2}$$

where θ_0 and θ are the installation angle of the system at initial and arbitrary positions respectively; L is the length of rod, x is the extension length of horizontal spring, and y is the vertical displacement.

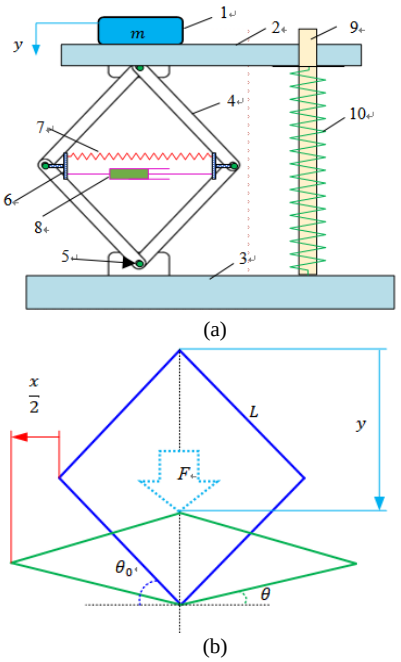

Fig. 1. Schematic diagram of proposed model. (a) X-shaped QZS isolator:1 – mass; 2 – support platform; 3 – base; 4 – rods; 5 – joints; 6 – end blocks; 7 – horizontal spring; 8 – damper; 9 – slide rial; 10 – vertical spring; (b) Deformation relationship.

When the support platform is vertically displaced under the action of a force, the potential energy V produced by the horizontal spring and vertical spring of the system can be obtained as

$$V = \frac{1}{2}k_s x^2 + \frac{1}{2}k_v y^2 \tag{3}$$

where k_s and k_v is the stiffness of horizontal spring and vertical spring respectively. By differentiating (3) with respect to y, and substituting (1) (2) into (3), the relation between restoring force F and vertical displacement y can be written as

$$F = \frac{dV}{dy} = k_s x\frac{dx}{dy} + k_v y = 2k_s L\left(\sin\theta_0 - \frac{y}{2L}\right) - 2k_s L\frac{\left(\sin\theta_0 - \frac{y}{2L}\right)\cos\theta_0}{\sqrt{1-\left(\sin\theta_0 - \frac{y}{2L}\right)^2}} + k_v y \tag{4}$$

For the convenience of subsequent research, defining $\hat{F} = F/(k_s L)$ is the dimensionless restoring force, $\hat{y} = y/L$ is dimensionless displacement, $\alpha = k_v/k_s$ is spring ratio. The expression of restoring force can be rewritten as

$$\hat{F} = 2\left(\sin\theta_0 - \frac{\hat{y}}{2}\right) - 2\frac{\left(\sin\theta_0 - \frac{\hat{y}}{2}\right)\cos\theta_0}{\sqrt{1-\left(\sin\theta_0 - \frac{\hat{y}}{2}\right)^2}} + \alpha\hat{y} \tag{5}$$

The nonlinear damping force F_d provided by horizontal damping in vertical direction can be expressed as

$$F_d = C\dot{x}\tan\theta = C\left(\frac{dx}{dy}\cdot\frac{dy}{dt}\right)\tan\theta = C\frac{\left(\sin\theta_0 - \frac{\hat{y}}{2}\right)^2}{1-\left(\sin\theta_0 - \frac{\hat{y}}{2}\right)^2}\dot{y} = C\hat{f}_d\dot{y} = f_d\dot{y} \tag{6}$$

where C is the horizontal damping coefficient; $\hat{f}_d$ is the dimensionless nonlinear damping function; $f_d = C\hat{f}_d$ is the equivalent nonlinear damping coefficient.

Based on Eq. (5), the proposed model's restoring force-displacement curve and stiffness-displacement curve at different initial installation angles is obtained and plotted in Fig. 2. The stiffness-displacement curve of the system can be obtained by the derivative of Eq. (5). When the dimensionless stiffness $\hat{k}$ is less than a small value k_{qzs} (e.g. $\hat{k} \le 0.2$ or $k \le 100N/m$), the system is defined to be within the range of QZS [9].

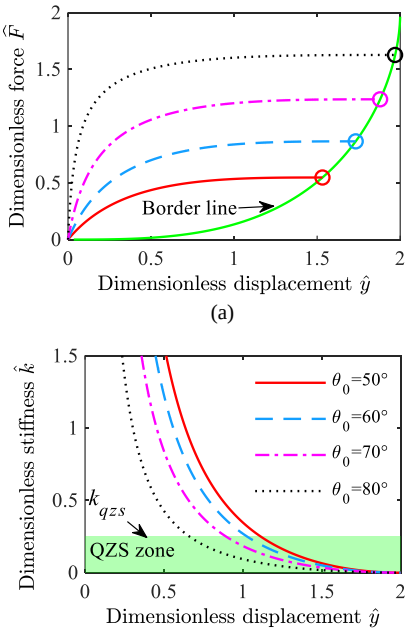

Fig. 2. The dimensionless force and stiffness versus displacement of proposed model with different initial angel. (a) Dimensionless force $\hat{F}$; (b) Dimensionless stiffness $\hat{k}$. "Solid line —" for $\theta_0 = 50°, \alpha = 0.36$; "Dash line --" for $\theta_0 = 60°, \alpha = 0.5$; "Dash dot line -·" for $\theta_0 = 70°, \alpha = 0.66$; "Dot line ···" for $\theta_0 = 80°, \alpha = 0.83$.

As shown in Fig. 2(a), the proposed model shows obvious asymmetric QZS characteristics. With the increase of initial installation angle, the bearing capacity of the system increases and the maximum stroke becomes longer. For the convenience of comparison, the maximum stroke points of the system under different angles are set to coincide in Fig. 2(b). It can be seen that the QZS range of the system increases with the increase of initial angle.

Fig. 3 shows the nonlinear damping characteristics of the system based on (6). As can be seen from Fig. 3, the equivalent nonlinear damping of proposed system has obvious asymmetric characteristics, which decrease with the increase of vertical displacement and increases with the increase of horizontal damping coefficient. The benefits of this nonlinear damping will be investigated in the next section of dynamic analysis.

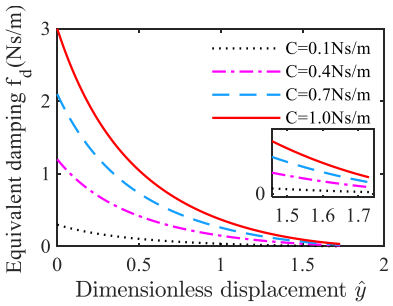

Fig. 3. Equivalent nonlinear damping properties of proposed model versus displacement and damping coefficients for $\theta_0 = 60°$.

IV. Dynamic Analysis

This section will discuss the dynamic response characteristics of the proposed asymmetric QZS system and the influence mechanism of geometrical nonlinear damping on the force transmissibility.

A. Dynamic Response

The system will produce a static displacement y_{st} under the action of the loaded mass *m*, which is the equilibrium position. Setting the equilibrium position to the origin, the dynamic displacement of the system is $y_e = y - y_{st}$. Under the action of harmonic force excitation $F_e = f\cos\omega t$ from the supported equipment, the motion equation of the system is obtained as

$$m\ddot{y}_e = -C\hat{f}_d\dot{y}_e - k_sL\hat{F}(y_e) + mg + f\cos\omega t \quad (7)$$

Defining $\omega_0 = \sqrt{k_s/m}$ as the natural frequency of proposed system, (7) can be can be deduced as

$$\frac{\ddot{y}_e}{\omega_0^2 L} = -\frac{C}{m\omega_0}\hat{f}_d\frac{\dot{y}_e}{\omega_0 L} - \hat{F}(y_e) + \frac{mg}{k_sL} + \frac{f}{mL\omega_0^2}\cos\left(\frac{\omega}{\omega_0}\omega_0 t\right) \quad (8)$$

In order to establish the dimensionless motion equation of proposed system to facilitate the subsequent analysis, we introduce the following parameters [2, 21]:

$$\Omega = \omega/\omega_0, \hat{y}_e = y_e/L, \tau = \omega_0 t, \quad \xi = C/(2m\omega_0), f_0 = f/(mL\omega_0^2) \quad (9)$$

where Ω is the dimensionless excitation frequency; $\hat{y}_e$ is the dimensionless dynamic displacement; ω is the excitation frequency; τ is the dimensionless time; ξ means the geometrical nonlinear damping ratio, f_0 is the dimensionless excitation amplitude.

Expanding the dimensionless restoring force and the nonlinear damping function by Taylor expansion at equilibrium position, and then substituting (9) into (8), the system's dimensionless motion equation can be written as

$$\hat{y}_e'' + (\chi_1\hat{y}_e + \chi_2\hat{y}_e^2 + \chi_3\hat{y}_e^3) + 2\xi(\eta_0 + \eta_1\hat{y}_e + \eta_2\hat{y}_e^2 + \eta_3\hat{y}_e^3)\hat{y}_e' = f_0\cos(\Omega\tau) \quad (10)$$

where χ_i, $\eta_i, i = (0, 1, 2, 3)$ is the Taylor expansion coefficients of $\hat{F}(y_e)$ and $\hat{f}_d(y_e)$ respectively, and $(\cdot)' = d(\cdot)/d\tau$, $\chi_0 = mg/(k_sL)$.

Considering only the primary harmonic response, the steady-state response of the system can be assumed as $\hat{y}_e = a_0 + a\cos(\Omega\tau + \varphi)$. Using the HBM, the response of proposed system can be solved as

$$\frac{3}{2}\chi_3 a_0 a^2 + \frac{1}{2}\chi_2 a^2 + \chi_3 a_0^3 + \chi_2 a_0^2 + \chi_1 a_0 = 0 \quad (11a)$$

$$-a\Omega^2 + a\left(\chi_3\left(\frac{3}{4}a^2 + 3a_0^2\right) + 2\chi_2 a_0 + \chi_1\right) = f_0\cos\varphi \quad (11b)$$

$$\xi_e a\Omega = f_0\sin\varphi \quad (11c)$$

$$\xi_e = 2\xi\left[\eta_3\left(\frac{3}{4}a_0 a^2 + a_0^3\right) + \eta_2\left(\frac{1}{4}a^2 + a_0^2\right) + \eta_1 a_0 + \eta_0\right] \quad (11d)$$

where ξ_e is the equivalent damping ratio of the system; a_0 is the offset of the response; a is the amplitude of the response; and φ is the phase of the response.

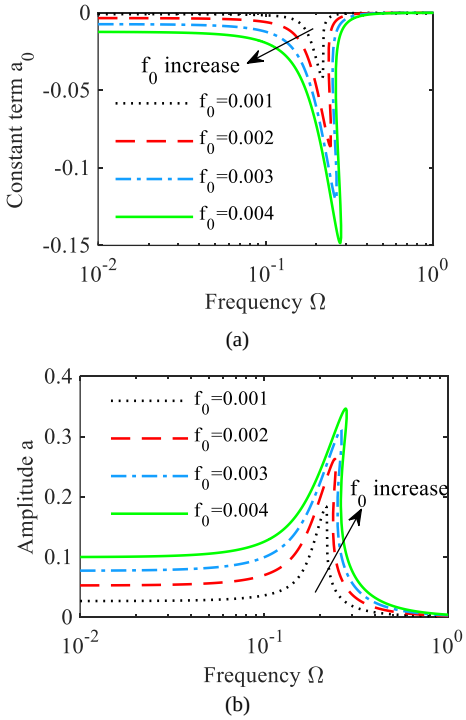

Fig. 4. The steady-state response of the system for different excitation amplitude with $\theta_0 = 60°, \alpha = 0.5, \xi = 0.2$. (a) constant component a_0; (b) resonance component a.

The steady-state response of proposed system varies with the excitation amplitude is solved based on (11) and

plotted in Fig. 4. It can be seen that with the increase of excitation amplitude, the system's response peak and corresponding frequency are also larger. The system shows the characteristics of hardening stiffness and jumping phenomena can be observed when the excitation is large. In addition, as the response of the system increases, the constant component a_0 becomes larger, and the system tends to oscillate in the negative direction of the equilibrium position, that is, the mass vibrates at a smaller vertical displacement $\hat{y}$.

B. Force Transmissibility

Force transmissibility T_f is the ratio between the force transmitted to the base and the excitation force, which can be expressed as

$$\begin{cases} T_f = \frac{1}{f_0}\sqrt{(2\xi_e a\Omega)^2 + \Lambda^2} \\ \Lambda = \chi_3\left(\frac{3}{4}a^3 + 3aa_0^2\right) + 2\chi_2 aa_0 + \chi_1 a \end{cases} \tag{12}$$

Fig. 5 shows the force transmissibility and the equivalent damping ratio of the system versus excitation frequency under different damping coefficients for $\theta_0 = 60°, f_0 = 0.002$.

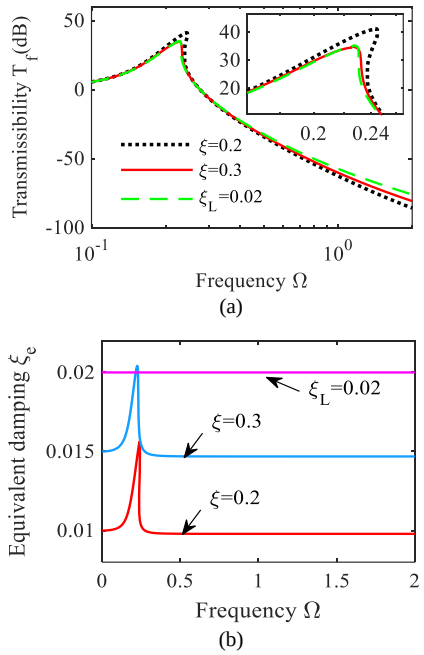

Fig. 5. Force transmissibility and equivalent damping ratio of the system under different damping coefficients for $\theta_0 = 60°, \alpha = 0.5, f_0 = 0.002$. (a) Force transmissibility; (b) equivalent damping ratio.

Note that Fig. 5 (a) is plotted based on (12) and Fig. 5 (b) is based on (11d). In order to compare the advantages of nonlinear geometric damping, the force transmissibility of vibration isolators with linear damping is also plotted. The linear damping represents the damping between the foundation and the platform, and its value remains constant during the vibration process. The linear damping ratio ξ_L is set to $\xi_L = 0.02$ in this paper. It can be seen that the system possesses good vibration isolation performance in low-frequency region. With the increase of the nonlinear damping ratio, the peak transmissibility and resonance frequency of the system decrease, that is, the resonance response of the system is suppressed. In addition, resonance can also be suppressed by setting linear damping ($\xi_L = 0.02$). Although the increase in nonlinear damping ratio ξ will reduce the vibration isolation effect in high-frequency region, as can be seen from Fig 5 (a), compared with using linear damping ξ_L, better high-frequency vibration isolation performance can be obtained by using the proposed nonlinear damping to suppress the resonance response.

The reason why geometrical nonlinear damping can achieve better vibration isolation is shown in Fig 5 (b). It can be seen that the equivalent nonlinear damping ratio ξ_e can reach the same magnitude as the linear damping ξ_L in the resonant region, but is much smaller than the linear damping in the high frequency region. Therefore, the nonlinear damping not only achieve the low-frequency resonance suppression, but also has a better high-frequency isolation effect. As previous analysis in this paper, the system response in the resonance region is large and the mass vibrates at a smaller vertical displacement $\hat{y}$. As can be seen from Fig 3, the nonlinear damping coefficients of the system increases with the decrease of displacement, therefore, the system exhibits a high equivalent damping ratio in the resonance region and the resonance will be effectively suppressed. The system response is small in high-frequency region, that is, the system exhibits small damping. At this time, the system has a smaller equivalent damping ratio and possesses better high-frequency vibration isolation performance.

C. Discussion

For symmetric QZS isolator, its force transmissibility in high frequency region will not decrease with the increase of geometric nonlinear damping [3, 21]. However, this result is not completely valid for asymmetric QZS system. Nevertheless, through the analysis in this paper, it can be conducted that the high-frequency transmissibility of asymmetric QZS system can still be reduced by increasing geometric nonlinear damping to suppress the resonance compared with increasing linear damping. As a result, geometrically nonlinear damping is still beneficial for asymmetric QZS isolator.

V. Conclusion

In this paper, a QZS isolator with asymmetrical stiffness and geometric nonlinear damping is proposed. The nonlinear stiffness and nonlinear damping characteristics of proposed model are studied. The motion equation of the system under force excitation is established, and its dynamic response is solved by HBM. Finally, the force transmissibility of the system under different damping coefficients is studied. The results indicate that the proposed isolator has the characteristics of asymmetric stiffness and asymmetric damping. The proposed system exhibits a large equivalent damping ratio in the resonance region and a small equivalent damping ratio in the high-frequency region, that is, the proposed QZS isolator can supress the resonance in low-frequency under force excitation and achieve a good high-frequency vibration isolation effect simultaneously than linear damping.

CONFLICT OF INTEREST

The authors declare no conflict of interest.

AUTHOR CONTRIBUTIONS

Chuanyun Yu: Conceptualization, Data Curation, Formal Analysis, Investigation, Methodology, Software, Validation, Visualization, Writing – Original Draft Preparation. Jianrun Zhang: Funding Acquisition, Project Administration, Resources, Supervision, Writing – Review and Editing. all authors had approved the final version.

FUNDING

This research is supported by the National Key Research and Development Program of China (Grant No. 2019YFB2006402)

REFERENCES

[1] R. A. Ibrahim, "Recent advances in nonlinear passive vibration isolators," *Journal of Sound and Vibration*, vol. 314, no. 3–5, pp. 371–452, 2008.

[2] Z. F. Hao, and Q. J. Cao, "The isolation characteristics of an archetypal dynamical model with stable-quasi-zero-stiffness," *Journal of Sound and Vibration*, vol. 340, pp. 61–79, 2015. https://doi.org/10.1016/j.jsv.2014.11.038

[3] C. Cheng, S. M. Li, Y. Wang, and X. J. Jing. "Force and displacement transmissibility of a quasi-zero stiffness vibration isolator with geometric nonlinear damping," *Nonlinear Dynamics*, vol. 87, pp. 2267–2279, 2017. https://doi.org/10.1007/s11071-016-3188-0

[4] X. Y. Hu, and C. Y. Zhou, "The effect of various damping on the isolation performance of quasi-zero-stiffness system," *Mechanical Systems and Signal Processing*, vol. 171, #108944, 2022.

[5] H. Li, Y. C. Li, and J. C. Li, "Negative stiffness devices for vibration isolation applications: A review," *Advances in Structural Engineering*, vol.23, no.8, pp. 1739–1755, 2020.

[6] A. Carrella, M. J. Brennan, and T. P. Waters, "Static analysis of a passive vibration isolator with quasi-zero-stiffness characteristic," *Journal of Sound and Vibration*, vol. 301, no. 3-5, pp. 678–689, 2007.

[7] Y. Sun, J. S. Zhou, D. Thompson, T. C. Yuan, D. Gong, and T. W. You, "Design, analysis and experimental validation of high static and low dynamic stiffness mounts based on target force curves," *International Journal of Non-Linear Mechanics*, vol. 126, #103559, 2020. https://doi.org/10.1016/j.ijnonlinmec.2020.103559

[8] B. Yan, H. Y. Ma, C. X. Zhao, C. Y. Wu, K. Wang *et al*., "A vari-stiffness nonlinear isolator with magnetic effects: Theoretical modeling and experimental verification," *International Journal of Mechanical Sciences*, vol. 148, pp. 745–755, 2018. https://doi.org/10.1016/j.ijmecsci.2018.09.031

[9] S. J. Yuan, Y. Sun, J. L. Zhao, K. Meng, M. Wang *et al*., "A tunable quasi-zero stiffness isolator based on a linear electromagnetic spring," *Journal of Sound and Vibration*, vol. 482, #115449, 2020.

[10] B. A. Fulcher, D. W. Shahan, M. R. Haberman, C. Conner Seepersad, and P. S. Wilson, "Analytical and experimental investigation of buckled beams as negative stiffness elements for passive vibration and shock isolation systems." *ASME: Journal of Vibration and Acoustics*, vol. 136, #031009, 2014.

[11] E. Palomares, A. J. Nieto, A. L. Morales, J. M. Chicharro, and P. Pintado, "Numerical and experimental analysis of a vibration isolator equipped with a negative stiffness system," *Journal of Sound and Vibration*, vol. 414, pp. 31–42, 2018. https://doi.org/10.1016/j.jsv.2017.11.006

[12] M. Li, Y. Q. Li, X. H. Liu, and F. H. Dai, "A quasi-zero-stiffness vibration isolator using bi-stable hybrid symmetric laminate," *Composite Structures*, vol. 299, #116047, 2022.

[13] J. Bian and X. J. Jing, "Superior nonlinear passive damping characteristics of the bio-inspired limb-like or X-shaped structure," *Mechanical Systems and Signal Processing*, vol. 125, pp. 21–51, 2019. https://doi.org/10.1016/j.ymssp.2018.02.014

[14] X. J. Jing, Y. Y. Chai, X. Chao, and J. Bian, "In-situ adjustable nonlinear passive stiffness using X-shaped mechanisms," *Mechanical Systems and Signal Processing*, vol. 170, #108267, 2022.

[15] Y. Wang and X. J. Jing, "Nonlinear stiffness and dynamical response characteristics of an asymmetric X-shaped structure," *Mechanical Systems and Signal Processing*, vol. 125, pp. 142–169, 2019. https://doi.org/10.1016/j.ymssp.2018.03.045

[16] X. T. Sun, X. J. Jing, J. Xu, and L. Cheng. "Vibration isolation via a scissor-like structured platform," *Journal of Sound and Vibration*, vol. 333, no. 9, pp. 2404–2420, 2014.

[17] X. T. Sun, F. Wang, and J. Xu, "A novel dynamic stabilization and vibration isolation structure inspired by the role of avian neck," *International Journal of Mechanical Sciences*, vol. 193, #106166, 2021.

[18] M. Shahraeeni, V. Sorokin, B. Mace, and S. Ilanko, "Effect of damping nonlinearity on the dynamics and performance of a quasi-zero-stiffness vibration isolator," *Journal of Sound and Vibration*, vol. 526, #116822, 2022.

[19] Z. K. Peng, G. Meng, Z. Q. Lang, W. M. Zhang, and F. L. Chu. "Study of the effects of cubic nonlinear damping on vibration isolations using harmonic balance method," *International Journal of Non-Linear Mechanics*, vol. 47, no. 10, pp.1073–1080, 2012.

[20] G. X. Dong, Y. H. Zhang, Y. J. Luo, S. L. Xie, and X. N. Zhang, "Enhanced isolation performance of a high-static–low-dynamic stiffness isolator with geometric nonlinear damping," *Nonlinear Dynamics*, vol. 93, pp. 2339–2356, 2018, https://doi.org/10.1007/s11071-018-4328-5

[21] C. R. Liu, K. P. Yu, and J. Tang, "New insights into the damping characteristics of a typical quasi-zero-stiffness vibration isolator," *International Journal of Non-Linear Mechanics*, vol. 124, #103511, 2020.

Chuanyun Yu received his master's degree in mechanical engineering in Southeast University in 2019, and is now studying for a doctorate in mechanical engineering at Southeast University, Nanjing, China. His areas of research include vibration control, mechanical dynamics and noise control.

Jianrun Zhang received his doctorate in mechanical engineering in Southeast University in 1997. Later, he conducted postdoctoral research in Italy's FIAT Research Center (Centro Ricerch Fiat) and the Institute of Acoustics (Technische Universitat Berlin, Institut für Technische Akustik, Germany). Now he is a professor in school of mechanical engineering at Southeast University, Nanjing, China. His main research fields are structural dynamics optimization, vibration and noise control, and vehicle dynamics.